Low temperature electron-phonon resonance in dc-current-biased two-dimensional electron systems

X. L. Lei
Department of Physics, Shanghai Jiaotong University, 1954 Huashan Road, Shanghai 200030, People's Republic of China
(Received 31 March 2008; published 12 May 2008)

Effects of resonant acoustic phonon scattering on magnetoresistivity are examined in two-dimensional electron systems at low temperatures by using a balance-equation magnetotransport scheme directly controlled by the current. The experimentally observed resonances in linear resistivity are shown to result from the conventional bulk phonon modes in a GaAs-based system without invoking leaky interface phonons. Due to quick heating of electrons, phonon resonances can be dramatically enhanced by a finite bias current. When the electron drift velocity increases to the speed of sound, additional and prominent phonon resonance peaks begin to emerge. As a result, remarkable resistance oscillation and negative differential resistivity can appear in nonlinear transport in a modest mobility sample at low temperatures, which is in agreement with recent experiments.

DOI: 10.1103/PhysRevB.77.205309 PACS number(s): 73.50.Jt, 73.40.−c

I. INTRODUCTION

Low temperature magnetoresistance oscillations related to linear and nonlinear transport of electrons in high Landau levels of high-mobility two-dimensional systems, induced by microwave radiation[1–9] or by direct current excitation,[10–17] have attracted a great deal of attention in the past few years. Despite the fact that detailed microscopic mechanisms are still under debate, there is almost no objection to refer these oscillatory magnetoresistances mainly to impurity or disorder scatterings, and the direct phonon contributions to resistivity are believed to be negligible in these systems at such low temperatures.

Recently, the magnetophonon resonance in semiconductors, previously known to result from electron coupling with optic phonons and can be observed only at high temperatures and high magnetic fields,[18,19] has been demonstrated to occur at temperatures as low as $T\sim 3$ K and lower magnetic fields in GaAs-based heterosystems.[20–23] The resonant magnetoresistance was detected and referred to as electron scatterings by two leaky interface phonon modes that have sound velocities $v_s \simeq 2.9$ km/s and $v_s \simeq 4.4$ km/s,[20–22] or by a single leaky interface phonon mode that has a velocity $v_s = 5.9$ km/s.[23] Very recently, Zhang *et al.*[24] found that acoustic phonon-induced resistance resonances are dramatically enhanced in the nonlinear dc response and a finite current can strongly modify the phonon resonance behavior, transforming resistance maxima into minima and back.[24] These phonon-related resistance oscillations remain poorly understood, especially the exact resonant condition, relative contributions of different modes, and how they are affected by temperature and current.

In this paper, we present a systematic analysis on nonlinear magnetotransport in GaAs-based semiconductors with a microscopic balance-equation scheme directly controlled by the current, which takes into account electron couplings with impurity, bulk longitudinal and transverse acoustic phonons, as well as polar optic phonons. Due to the quick rise of electron temperature, the phonon resonances are dramatically enhanced by a finite current. When electron drift velocity v gets into the supersonic regime ($v \geq v_s$, the speed of sound), additional magnetophonon resonance peaks emerge. As a result, a remarkable resistance oscillation and a negative differential resistivity appear in the nonlinear magnetotransport in a modest mobility sample at low temperatures.

II. BALANCE EQUATIONS FOR NONLINEAR MAGNETOTRANSPORT

We consider a quasi-two-dimensional system consisting of N_s electrons in a unit area of an x-y plane. These electrons, subjected to a uniform magnetic field $\boldsymbol{B}=(0,0,B)$ along the z direction and a uniform electric field $\boldsymbol{E}$ in the x-y plane, are scattered by random impurities and by phonons in the lattice. In terms of the center-of-mass momentum and coordinate defined as $\boldsymbol{P}\equiv\Sigma_j \boldsymbol{p}_{j\|}$ and $\boldsymbol{R}\equiv N_s^{-1}\Sigma_j \boldsymbol{r}_j$, with $\boldsymbol{p}_{j\|}\equiv(p_{jx},p_{jy})$ and $\boldsymbol{r}_j\equiv(x_j,y_j)$ being the momentum and coordinate of the jth electron in the plane, and the relative electron momentum and coordinate $\boldsymbol{p}'_{j\|}\equiv\boldsymbol{p}_{j\|}-\boldsymbol{P}/N_s$ and $\boldsymbol{r}'_j\equiv\boldsymbol{r}_j-\boldsymbol{R}$, the Hamiltonian H of this coupled electron-phonon system can be written as the sum of a center-of-mass part $H_{\rm cm}$, a relative electron part $H_{\rm er}$,[25–28]

$$H_{\rm cm}=\frac{1}{2N_s m}[\boldsymbol{P}-N_s e\boldsymbol{A}(\boldsymbol{R})]^2-N_s e\boldsymbol{E}\cdot\boldsymbol{R}, \tag{1}$$

$$H_{\rm er}=\sum_j\left\{\frac{1}{2m}[\boldsymbol{p}'_{j\|}-e\boldsymbol{A}(\boldsymbol{r}'_j)]^2+\frac{p_{jz}^2}{2m_z}+V(z_j)\right\}+\sum_{i<j}V_c(\boldsymbol{r}'_i-\boldsymbol{r}'_j,z_i,z_j), \tag{2}$$

and a phonon part $H_{\rm ph}=\Sigma_{\boldsymbol{q}\lambda}\Omega_{\boldsymbol{q}\lambda}b^\dagger_{\boldsymbol{q}\lambda}b_{\boldsymbol{q}\lambda}$, together with electron-impurity and electron-phonon interactions as follows:

$$H_{\rm ei}=\sum_{\boldsymbol{q}_\|,a}u(\boldsymbol{q}_\|,z_a)e^{-i\boldsymbol{q}_\|\cdot\boldsymbol{r}_a}e^{i\boldsymbol{q}_\|\cdot\boldsymbol{R}}\rho_{\boldsymbol{q}_\|}, \tag{3}$$

$$H_{\rm ep} = \sum_{\boldsymbol{q},\lambda} M(\boldsymbol{q},\lambda) I(q_z)(b_{\boldsymbol{q}\lambda} + b^{\dagger}_{-\boldsymbol{q}\lambda}) e^{i\boldsymbol{q}_{\parallel}\cdot\boldsymbol{R}} \rho_{\boldsymbol{q}_{\parallel}}. \tag{4}$$

Here, $\boldsymbol{A}(\boldsymbol{r})$, the in-plane component of the vector potential of the uniform magnetic field, is linear in the spatial coordinate $\boldsymbol{r}=(x,y)$; m and m_z are, respectively, the electron effective mass parallel and perpendicular to the plane; $V(z)$ and $V_c(\boldsymbol{r}'_i-\boldsymbol{r}'_j,z_i,z_j)$ stand for the confined and Coulomb potentials, respectively; $\rho_{\boldsymbol{q}_{\parallel}}=\Sigma_j e^{i\boldsymbol{q}_{\parallel}\cdot\boldsymbol{r}'_{j\parallel}}$ is the density operator of the two-dimensional (2D) relative electrons; $u(\boldsymbol{q}_{\parallel},z_a)$ is the effective potential of the ath impurity located at $(\boldsymbol{r}_a,z_a)$ in the 2D Fourier space; $b^{\dagger}_{\boldsymbol{q}\lambda}(b_{\boldsymbol{q}\lambda})$ is the creation (annihilation) operator of the bulk phonon with wave vector $\boldsymbol{q}=(\boldsymbol{q}_{\parallel},q_z)=(q_x,q_y,q_z)$ in branch λ that has an energy $\Omega_{\boldsymbol{q}\lambda}$; $M(\boldsymbol{q},\lambda)$ is the matrix element of the electron-phonon interaction in the three-dimensional (3D) plane-wave representation; and $I(q_z)$ is a form factor of the quasi-2D electron.[27] Here, for simplicity, we have assumed that the quasi-2D electrons occupy only the lowest subband and, thus, the subband summation indices in Eqs. (3) and (4) are neglected.[27]

The separation of the electron Hamiltonian into a center-of-mass part and a relative electron part amounts to looking at electrons in a reference frame moving with their center of mass. The most important feature of this separation is that a spatially uniform electric field shows up only in $H_{\rm cm}$, and that $H_{\rm er}$ is the Hamiltonian of a many particle system subject to a perpendicular magnetic field *without the electric field*. This enables us to deal with relative electrons in the magnetic field *without tilting the Landau levels*. The coupling between the center of mass and relative electrons is shown by the factor $e^{i\boldsymbol{q}_{\parallel}\cdot\boldsymbol{R}}$ inside the momentum summation in $H_{\rm ei}$ and $H_{\rm ep}$. The moving center-of-mass assisted transitions of relative electrons between different Landau levels provide the major mechanism for the current-driven magnetotransport.

Our treatment starts with the Heisenberg operator equations for the rate of change in the center-of-mass velocity $\boldsymbol{V}=-i[\boldsymbol{R},H]$ and that for the relative electron energy $H_{\rm er}$ as follows:

$$\dot{\boldsymbol{V}} = -i[\boldsymbol{V},H], \tag{5}$$

$$\dot{H}_{\rm er} = -i[H_{\rm er},H]. \tag{6}$$

When the electron-impurity and electron-phonon couplings are weak in comparison with the internal thermalization of relative electrons and that of phonons, it is good enough to carry out the statistical average of the above operator equations to leading orders in $H_{\rm ei}$ and $H_{\rm ep}$. For this purpose, we only need to know the distribution of relative electrons and phonons without being perturbed by $H_{\rm ei}$ or $H_{\rm ep}$. The distribution function of the relative electron system described by Hamiltonian (2) without an electric field should be an isotropic Fermi-type function with a single temperature T_e. The phonon system, which is assumed to be in an equilibrium state, has a Bose distribution with lattice temperature T. Such a statistical average of the above operator equations yields the following force and energy balance equations in the steady state, which has a constant average drift velocity $\boldsymbol{v}$:

$$N_s e\boldsymbol{E} + N_s e(\boldsymbol{v}\times\boldsymbol{B}) + \boldsymbol{f}(\boldsymbol{v}) = 0, \tag{7}$$

$$\boldsymbol{v}\cdot\boldsymbol{f}(\boldsymbol{v}) + w(\boldsymbol{v}) = 0. \tag{8}$$

Here, $\boldsymbol{f}(\boldsymbol{v})=\boldsymbol{f}_i(\boldsymbol{v})+\boldsymbol{f}_p(\boldsymbol{v})$ is the frictional force experienced by the electron center of mass due to impurity and phonon scatterings, given by

$$\boldsymbol{f}_i(\boldsymbol{v}) = \sum_{\boldsymbol{q}_{\parallel}} \boldsymbol{q}_{\parallel} |U(\boldsymbol{q}_{\parallel})|^2 \Pi_2(\boldsymbol{q}_{\parallel},\omega_0), \tag{9}$$

$$\boldsymbol{f}_p(\boldsymbol{v}) = 2\sum_{\boldsymbol{q},\lambda} \boldsymbol{q}_{\parallel} |M(\boldsymbol{q},\lambda)|^2 |I(q_z)|^2 \Pi_2(\boldsymbol{q}_{\parallel},\Omega_{\boldsymbol{q}\lambda}+\omega_0) \times \left[n\left(\frac{\Omega_{\boldsymbol{q}\lambda}}{T}\right) - n\left(\frac{\Omega_{\boldsymbol{q}\lambda}+\omega_0}{T_e}\right)\right], \tag{10}$$

and $w(\boldsymbol{v})$ is the electron energy-loss rate to the lattice due to electron-phonon interactions with an expression obtained from the right-hand side of Eq. (10) by replacing the $\boldsymbol{q}_{\parallel}$ factor with $\Omega_{\boldsymbol{q}\lambda}$. In these equations, $\omega_0\equiv\boldsymbol{q}_{\parallel}\cdot\boldsymbol{v}$, $|U(\boldsymbol{q}_{\parallel})|^2$ is the effective average impurity scattering potential, and $|M(\boldsymbol{q},\lambda)|^2|I(q_z)|^2$ is the effective coupling matrix element between a λ-branch 3D phonon and a quasi-2D electron, $\Pi_2(\boldsymbol{q}_{\parallel},\Omega)$ is the imaginary part of the 2D electron density correlation function at electron temperature T_e in the presence of the magnetic field, and $n(x)\equiv 1/(e^x-1)$ is the Bose function. The effect of interparticle Coulomb interaction is included in the density correlation function to the degree of electron level broadening and screening. With the screening statically considered in the effective impurity and phonon potentials, the remaining $\Pi_2(\boldsymbol{q}_{\parallel},\Omega)$ function in Eqs. (9) and (10) is that of a noninteracting 2D electron gas in the magnetic field, which can be written in the Landau representation as[25]

$$\Pi_2(\boldsymbol{q}_{\parallel},\Omega) = \frac{1}{2\pi l_{\rm B}^2}\sum_{n,n'} C_{n,n'}(l_{\rm B}^2 q_{\parallel}^2/2)\Pi_2(n,n',\Omega), \tag{11}$$

$$\Pi_2(n,n',\Omega) = -\frac{2}{\pi}\int d\varepsilon [f(\varepsilon)-f(\varepsilon+\Omega)] \times {\rm Im}\, G_n(\varepsilon+\Omega){\rm Im}\, G_{n'}(\varepsilon), \tag{12}$$

where $l_B=\sqrt{1/|eB|}$ is the magnetic length, $C_{n,n+l}(Y)\equiv n![(n+l)!]^{-1}Y^l e^{-Y}[L_n^l(Y)]^2$ with $L_n^l(Y)$ the associate Laguerre polynomial, $f(\varepsilon)=\{\exp[(\varepsilon-\mu)/T_e]+1\}^{-1}$ is the Fermi function at electron temperature T_e, and Im $G_n(\varepsilon)$ is the density of states of the broadened Landau level n.

We model the electron density-of-states function with a Gaussian-type form for both overlapped and separated Landau levels ($\varepsilon_n=n\omega_c$ is the center of the nth Landau level; $\omega_c=eB/m$ is the cyclotron frequency[29] as follows:

$${\rm Im}\, G_n(\varepsilon) = -(2\pi)^{1/2}\Gamma^{-1}\exp[-2(\varepsilon-\varepsilon_n)^2/\Gamma^2]. \tag{13}$$

The half-width Γ, or the lifetime or the quantum scattering time, $\tau_s=1/2\Gamma$, of the Landau level, which should be determined by electron-impurity, electron-phonon, and electron-electron scatterings in the system, is magnetic-field B and temperature T dependent. We treat it as a semiempirical pa-

rameter, which will serve as the only adjustable parameter in the present investigation.

At lattice temperature T, the energy balance [Eq. (8)] yields the electron temperature T_e for a given carrier drift velocity $\boldsymbol{v}$ at a given magnetic field. Then, with this T_e, the force balance [Eq. (7)] determines the relation between $\boldsymbol{v}$, $\boldsymbol{B}$, and $\boldsymbol{E}$, i.e., the longitudinal and transverse resistivities in the magnetotransport.

Such a formulation indicates that the carrier drift velocity $\boldsymbol{v}$ is the basic physical quantity that controls the nonlinear magnetotransport. The frictional force $\boldsymbol{f}(\boldsymbol{v})$ and energy dissipation rate $w(\boldsymbol{v})$ solely depend on the drift velocity $\boldsymbol{v}$ at a given magnetic field B, while the electric field only plays a role in balancing the frictional force. Thus, the resistivity is directly determined by the scattering mechanisms and by the drift velocity or the current density, rather than by the electric field. Equations (7) and (8) are conveniently applied to current-driven magnetotransport of any configuration, in which the current is an experimentally directly controlled quantity. For an isotropic system where the frictional force is in the opposite direction of the drift velocity $\boldsymbol{v}$ and the magnitudes of both the frictional force and the energy-loss rate depend only on $v \equiv |\boldsymbol{v}|$, we can write $\boldsymbol{f}(\boldsymbol{v}) = f(v)\boldsymbol{v}/v$ and $w(\boldsymbol{v}) = w(v)$. In the Hall configuration with velocity $\boldsymbol{v}$ in the x direction [$\boldsymbol{v} = (v, 0, 0)$] or the current density $J_x = J = N_s e v$ and $J_y = 0$, Eq. (7) gives, after T_e [thus, the $f(v)$ function] determined from Eq. (8), $vf(v) + w(v) = 0$, the transverse resistivity $R_{yx} = B/N_s e$, and the longitudinal resistivity R_{xx} and the longitudinal differential resistivity r_{xx} as

$$R_{xx} = -f(v)/(N_s^2 e^2 v), \tag{14}$$

$$r_{xx} = -(\partial f(v)/\partial v)/(N_s^2 e^2). \tag{15}$$

Note that, in principle, since the Landau-level broadening and electron temperature are determined by the simultaneous existence of all of the scattering mechanisms, contributions to the total resistivity from different scattering mechanisms are not independent. Nevertheless, it is still useful to formally write the total resistivity as a direct sum of separate scattering contributions by the respective components of the frictional force $\boldsymbol{f}(\boldsymbol{v})$.

III. MAGNETOPHONON RESONANCE IN LINEAR MAGNETORESISTANCE

In the numerical analysis, we first concentrate on a GaAs-based heterosystem with carrier sheet density $N_s = 4.8 \times 10^{15}$ m^{-2} and zero-temperature linear mobility $\mu_0 = 440$ m^2/V s in the absence of a magnetic field, considering electron scatterings from bulk longitudinal acoustic (LA) phonons (one branch, via the deformation potential and piezoelectric couplings with electrons) and transverse acoustic (TA) phonons (two branches, via the piezoelectric coupling with electrons), as well as from remote and background impurities. The coupling matrix elements are taken to be well known expressions[27] with typical material parameters in bulk GaAs: electron effective mass $m = 0.067 m_e$ (m_e is the free electron mass), longitudinal sound velocity $v_{sl} = 5.29 \times 10^3$ m/s, transverse sound velocity $v_{st} = 2.48 \times 10^3$ m/s,

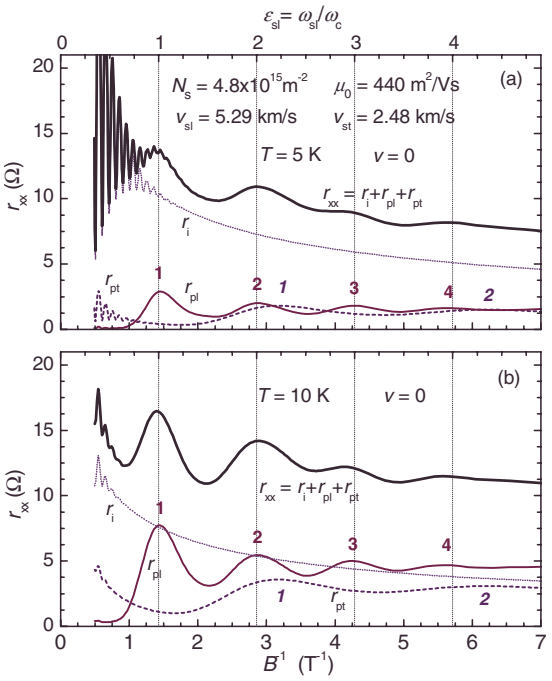

FIG. 1. (Color online) Linear ($v = 0$) resistivities (r_{xx}, r_i, r_{pl}, and r_{pt}) at (a) $T = 5$ K and (b) $T = 10$ K for a GaAs-based heterosystem with carrier sheet density $N_s = 4.8 \times 10^{15}$ m^{-2} and zero-temperature linear mobility $\mu_0 = 440$ m^2/V s. The longitudinal and transverse sound velocities are taken to be $v_{sl} = 5.29 \times 10^3$ m/s and $v_{st} = 2.48 \times 10^3$ m/s, respectively.

acoustic deformation potential $\Xi = 8.5$ eV, piezoelectric constant $e_{14} = 1.41 \times 10^9$ V/m, dielectric constant $\kappa = 12.9$, and material mass density $d = 5.31$ g/cm^3. We take a magnetic-field-dependent ($B^{1/2}$) Landau-level half-width as follows:

$$\Gamma = [8\alpha e \omega_c / \pi m \mu_0(T)]^{1/2}, \tag{16}$$

which is expressed in terms of $\mu_0(T)$, the total linear mobility at lattice temperature T in the absence of the magnetic field, and a broadening parameter α to take into account the difference in the transport scattering time from the broadening-related quantum lifetime.[2,4] A broadening parameter $\alpha = 1.5$ is used in the calculation in Secs. III and IV, which corresponds to taking Landau-level half-widths of $\Gamma = 1.8$ and 2.4 K, respectively, at lattice temperatures of $T = 5$ and 10 K for magnetic field $B = 0.5$ T.

The calculated total linear ($v \to 0$) magnetoresistivity (differential resistivity) $R_{xx} = r_{xx}$ is shown versus $1/B$ at lattice temperatures $T = 5$ K and $T = 10$ K in Figs. 1(a) and 1(b), together with separated contributions r_i from impurities, r_{pl} from LA phonons, and r_{pt} from TA phonons: $r_{xx} = r_i + r_{pl} + r_{pt}$. The resistivity resonances clearly appear in r_{pl} and r_{pt} at both temperatures. This feature of magnetoresistivity stems from the property of 2D electron density correlation function $\Pi_2(\boldsymbol{q}_\parallel, \Omega_{\boldsymbol{q}\lambda})$. In the case of low temperature (T_e much less than the Fermi energy ε_F) and large Landau-level filling factor ($\nu = \varepsilon_F/\omega_c \gg 1$), $\Pi_2(\boldsymbol{q}_\parallel, \Omega)$ is a periodic function with respect to its frequency variable: $\Pi_2(\boldsymbol{q}_\parallel, \Omega + l\omega_c) = \Pi_2(\boldsymbol{q}_\parallel, \Omega)$ for any integer l of $|l| \ll \nu$. On the other hand, under the same conditions (low temperature $T_e \ll \varepsilon_F$ and large filling factor

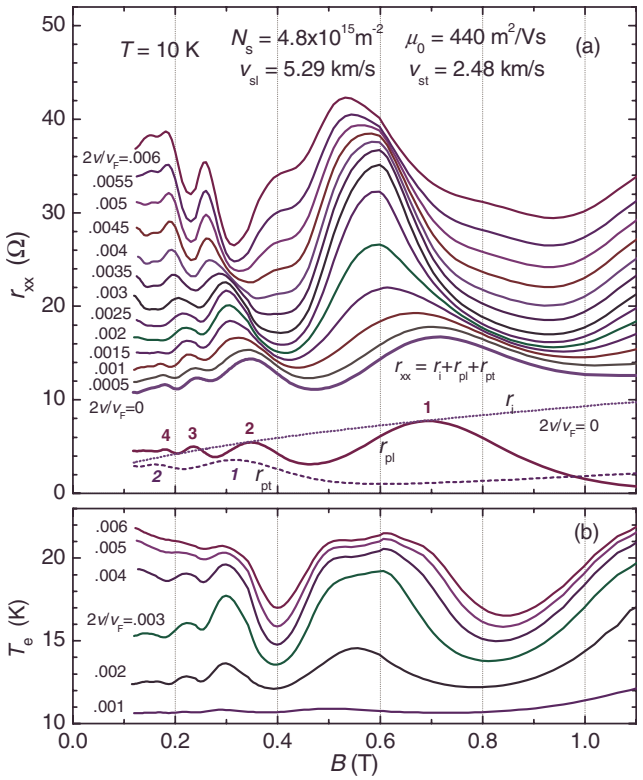

FIG. 2. (Color online) (a) Differential resistivities r_{xx} and (b) electron temperature T_e are shown as functions of the magnetic-field strength B at lattice temperature $T=10$ K under different values of the bias drift velocity v/v_F. Here, v_F is the Fermi velocity of the 2D electron system, and r_{xx} curves of different $2v/v_F$ values are vertically offset for clarity.

$\nu \gg 1$), the major contributions to the summation in Eq. (11) come from terms $n \sim n' \sim \nu$, and then the function $C_{n,n'}(x)$ has a sharp principal maximum near $x=4\nu$.[30,31] Therefore, as a function of the in-plane momentum $q_\parallel$, $\Pi_2(\boldsymbol{q}_\parallel,\Omega)$ sharply peaks at around $q_\parallel \simeq 2k_F$. In view of the existence of the form factor $|I(q_z)|^2$, which is related to the wave function of the quasi-2D electron, only very small q_z ($\ll k_F$) can contribute to the integration in Eq. (10), and thus, the contribution of the wave vector integration to the phonon-induced frictional force heavily weighs around $q \simeq 2k_F$. As a result of this phase-space weight distribution and the 3D phonon dispersion $[\Omega_{\boldsymbol{q}\lambda}=v_{s\lambda}q(\lambda=1,t)]$ when $\omega_{s\lambda} \equiv 2k_F v_{s\lambda} = l\omega_c$ ($l=1,2,3,\ldots$), a quasi-2D relative electron in any Landau level can be resonantly scattered by absorbing or emitting a phonon and jumps across l Landau levels. The linear resistivity maxima then show up at

$$\varepsilon_{s\lambda} \equiv \omega_{s\lambda}/\omega_c = l = 1,2,3,\ldots . \tag{17}$$

This is exactly what is seen in Figs. 1(a) and 1(b) as well as in the lower part of Fig. 2(a), where the $r_{\rm pl}$ maxima located at $\varepsilon_{\rm sl}=1,2,3,4$ and $r_{\rm pt}$ maxima at $\varepsilon_{\rm st}=1,2$ are labeled. The total resistivity r_{xx} peaks at around $\varepsilon_{\rm sl}=1,2,3,4$, which is essentially determined by the resonant scattering of LA phonons. These results are in good agreement with experiments,[23,24] which indicates that the observed low temperature magnetophonon resonances in linear magnetoresistance are well explained by the ordinary single bulk LA phonon mode in GaAs with no need to invoke leaky interface modes.

IV. MAGNETOPHONON RESONANCE IN NONLINEAR TRANSPORT

A finite current density J or a finite drift velocity v in the x direction has two major effects. First, it results in electron heating and thus raises the rate of phonon emission. As a result, the phonon contributed resistivity and the oscillatory amplitude of magnetophonon resonance is enhanced with increasing bias current density. The electron temperature is determined by the frictional force $f(v)$ and the energy-dissipation rate $w(v)$ through the energy balance [Eq. (8)]. Generally, longitudinal acoustic phonons give the dominant contribution to $w(v)$ in GaAs-based systems at lattice temperatures considered in this paper ($T \leq 10$ K), and the polar optic (LO) phonons are usually frozen. However, electron scattering from LO phonons should still be taken into account when the bias current density becomes strong that electron temperature T_e rises up to the order of 20 K, at which a weak emission of LO phonons can take place. These emitted LO phonons, although giving little contribution to the resistivity itself, provide an additional efficient energy-dissipation channel to prevent the continuing rise in electron temperature.[32] Therefore, we take the LO-phonon scattering (via the Fröhlich coupling electrons, with an optical dielectric constant $\kappa_\infty=10.5$) into account in the numerical calculation in nonlinear transport. The calculated electron temperatures T_e in the case of $T=10$ K at different bias drift velocities $2v/v_F=0.001$, 0.002, 0.003, 0.004, 0.005, and 0.006 (v_F is the Fermi velocity of the 2D electron system), which correspond to current densities $J=0.115$, 0.231, 0.346, 0.462, 0.577, and 0.693 A/m, are shown in Fig. 2(b) versus the magnetic field B for the GaAs heterosystem introduced above.

We see that, in addition to the concordant rise in electron temperature with increasing current density, at each bias drift velocity, T_e also exhibits resonance when changing magnetic field. The oscillatory peak-valley structure of T_e periodically shows up, which has a period $\Delta(\omega_{\rm sl}/\omega_c) \approx 1$, indicating that it is also a magnetophonon resonance mainly due to LA phonons. This T_e resonance stems from the periodicity of $f(v)$ and $w(v)$ functions in the energy balance equation (8). Note that when the bias current density grows, the oscillatory amplitude of T_e generally increases, but the positions of T_e peaks (valleys) remain essentially the same on the B axis. By comparing with the magnetophonon resonant linear resistivity r_{xx} [shown in the lower part of Fig. 2(a)], the oscillatory structure of T_e peaks (valleys) appears roughly $\pi/2$ phase shift down along the B axis.

The differential resistivity r_{xx} of the system at a given bias drift velocity v is obtained from the $\partial f(v)/\partial v$ function through Eq. (15), with the electron temperature T_e determined above. Since the peak (valley) positions of T_e are essentially fixed in the B axis, the variation of the resistivity maxima (minima) with changing bias velocity v is mainly determined by its direct effect in the $\partial f(v)/\partial v$ function, as

reflected in the frequency shift $\omega_0 \equiv \boldsymbol{q}_\parallel \cdot \boldsymbol{v}$ in the argument of the electron density correlation function. Physically, because an extra energy $\boldsymbol{q}_\parallel \cdot \boldsymbol{v}$ is provided by the moving center of mass to the relative electrons during the scattering process, the transition rate of an electron from Landau level n to n' (n' can be equal to or not equal to n) experiences a change due to impurity and phonon scatterings, which shows up through the $-\boldsymbol{q}_\parallel \cdot \boldsymbol{v}$ shift in, for instance, the $\Pi_2(\boldsymbol{q}_\parallel, \Omega_{\boldsymbol{q}\lambda} - \boldsymbol{q}_\parallel \cdot \boldsymbol{v})$ function in $-f_p$ (i.e., the resistivity). The effect of such an energy shift in the impurity scattering case has been shown to induce an oscillatory differential magnetoresistance r_i that is controlled by the following parameter:[10,12,14]

$$\varepsilon_j \equiv \omega_j/\omega_c, \quad \omega_j \equiv 2k_F v = \sqrt{8\pi/N_s} J/e, \tag{18}$$

which has peak positions at around $\varepsilon_j \approx 0, 1, 2, \ldots$. In the case of acoustic phonon scatterings, the resistivity maxima are expected to occur near the possible integer values of parameter $\varepsilon_{s\lambda} - \varepsilon_j$, i.e.,

$$\varepsilon_{s\lambda} - \varepsilon_j \approx l = 0, \pm 1, \pm 2, \ldots, \tag{19}$$

and this integer can be used as an identification for each magnetophonon resonance peak of the differential resistivity in nonlinear transport. When drift velocity v is smaller than the sound speed $v_{s\lambda}$ ($\varepsilon_j < \varepsilon_{s\lambda}$), the resonance condition (19) can be satisfied only for positive integers $l = 1, 2, 3, 4, \ldots$, whence the effect of a small current J is roughly to change the resistivity maxima from $\varepsilon_{s\lambda} \approx l$ in the linear case to

$$\varepsilon_{s\lambda} \approx l + \varepsilon_j. \tag{20}$$

This means that for a given index number l, the peak position of magnetophonon resonance moves toward lower B with increasing current density, and for a given J, the shifts of peak positions in the $\varepsilon_{s\lambda}$ axis are larger for larger index l (lower B field). These features are clearly seen in Fig. 2(a), where we show the calculated differential resistivity r_{xx} as a function of the magnetic field at $T = 10$ K under different bias drift velocities from $2v/v_F = 0$ to 0.006 in steps of 0.0005, corresponding to current densities $J = 0 - 0.693$ A/m in steps of 0.058 A/m. We see that though within certain v and B-field ranges, e.g., $2v/v_F = 0.003 \sim 0.005$ and B is around 6 T, the peak positions of the resistivity may be somewhat influenced by the rapid change in the electron temperature because of the enhanced phonon contributions at higher T_e; the main trend of the resistivity peak shift with increasing J remains. The progress and movement of respective peaks compare favorably with recent experimental observation.[24]

When v becomes equal to or greater than the sound speed $v_{s\lambda}$, the condition (19) can be satisfied by $l = 0$ and negative integers, which indicates the occurrence of additional magnetophonon resonance peaks under a strong dc excitation. Figure 3 presents the calculated differential resistivity r_{xx} and electron temperature T_e at the lattice temperature $T = 5$ K as functions of the current density in terms of $\varepsilon_j \equiv \omega_j/\omega_c$ at magnetic fields $B = 0.27$, 0.35, 0.47, and 0.72 T. Due to the rapid rise in electron temperature T_e in this $\mu_0 = 440$ m^2/V s system, acoustic phonon contribution to resistivity becomes significant when $\varepsilon_j > 0.1$. The prominent oscillations show up in resistivities r_i, $r_{\rm pl}$, $r_{\rm pt}$, and r_{xx}, all exhibiting a main oscillation period $\Delta\varepsilon_j \sim 1$. However, since the peak positions of LA and TA phonon resistivities $r_{\rm pl}$ and $r_{\rm pt}$ in the ε_j axis change with changing magnetic field, as indicated by condition (19) ($\varepsilon_j \approx \varepsilon_{s\lambda} - l$), the oscillating behavior of total resistivity r_{xx} is strongly B-field dependent. For instance, in the case of $B = 0.35$ T, the LA phonon resonance peaks 1, 0, −1, and −2 are essentially in phase with the TA phonon resonance peaks 0, −1, −2, and −3, and close to the maxima of the impurity resistivity r_i near $\varepsilon_j = 1, 2, 3, 4$, which lead to an enhanced r_{xx} with maxima around these positions [Fig. 3(c)]. In the case of $B = 0.47$ T, where the LA resonance peaks 1, 0, −1, and −2 are around $\varepsilon_j = 0.5$, 1.5, 2.5, and 3.5, and the TA resonance peaks 0, −1, −2, and −3 are around $\varepsilon_j = 0.7$, 1.7, 2.7, and 3.7, the resulting r_{xx} oscillation is out of phase with that of r_i oscillation and has secondary extremes [Fig. 3(b)]. As a result, at fixed ε_j, e.g., $\varepsilon_j = 2$, r_{xx} exhibits maxima for $B = 0.35$ and 0.72 T, while minima for $B = 0.27$ and 0.47 T. Note that the resonant magnetophonon resistivity at $v = v_{s\lambda}$ (the $l = 0$ peak) is generally the largest among all of the resistivity maxima in each type of phonon scattering, as can be seen from all four cases in Fig. 3. It comes from phonon-induced intra-Landau-level scatterings of electrons, which are allowed for all of the wave vectors, with the energy provided by the center of mass that has velocity $v = v_{s\lambda}$.

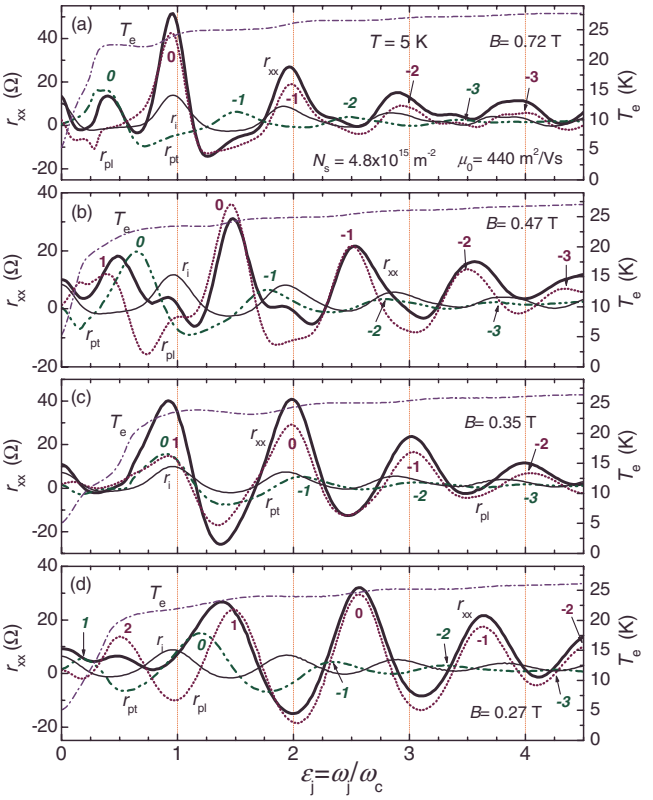

FIG. 3. (Color online) Differential resistivities (r_i, $r_{\rm pl}$, $r_{\rm pt}$, and r_{xx}) and electron temperature T_e are shown as functions of ε_j at fixed magnetic fields $B = 0.27$,0.35, 0.47, and 0.72 T, respectively, at $T = 5$ K. The number near the peak of $r_{\rm pl}$ or $r_{\rm pt}$ is the value of the integer l in the resonance condition (19) of the corresponding differential resistivity peak.

At fixed ε_j, phonon-induced resistivity is periodic in inverse B field with period $\Delta\varepsilon_{s\lambda} \approx 1$. The total resistivity r_{xx}

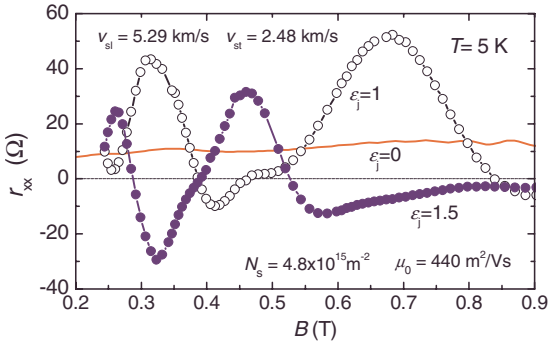

FIG. 4. (Color online) Differential resistivity r_{xx} is plotted versus magnetic field B for fixed values of ε_j=0, 1, and 1.5 at T=5 K.

roughly follows this rule, as shown in Fig. 4, where r_{xx} is plotted versus B for fixed ε_j=1 and 1.5. Both curves show remarkable oscillations that have the same periodicity but in and out of phase as that of the zero-bias (ε_j=0) case and with much enhanced amplitudes. These features are just those observed in the experiments.[24]

V. LOWER MOBILITY SYSTEMS

Magnetophonon resonance can show up in resistivity at even lower lattice temperature as long as a finite current density is applied. In a system with lower mobility, the phonon contributions to resistivity can be greatly enhanced by a modest finite current due to the rapid rise in the electron temperature.

As another example, Fig. 4 plots the total absolute resistivity R_{xx} and total differential resistivity r_{xx} and their respective contributions from impurity, LA phonons, and TA phonons (R_i and r_i, $R_{\rm pl}$ and $r_{\rm pl}$, and $R_{\rm pt}$ and $r_{\rm pt}$), and the electron temperature T_e as functions of bias current density in terms of ε_j at lattice temperature T=2 K and magnetic field B=0.51 T for a GaAs-based heterosystem that has carrier sheet density $N_s=8\times10^{15}$ m^{-2} and zero-temperature linear mobility μ_0=80 m^2/V s in the absence of magnetic field. The Landau-level half-width Γ is taken to be 1.3 K ($2\Gamma\approx0.25\omega_c$ at this magnetic field).

Note that the phonon-induced absolute resistivities $R_{\rm pl}$ and $R_{\rm pt}$ can become negative in this case. Although the total resistivity R_{xx} remains always positive, the growing negative $r_{\rm pl}$ and $r_{\rm pt}$ with increasing current density at the initial stage greatly accelerate the drop in the total differential resistivity such that r_{xx} goes down and become negative at $\varepsilon_j\approx0.07$, which is much smaller than it would be without phonon contribution ($\varepsilon_j\approx0.14$), solely determined by the width of the Landau level.[14] As a result, the total differential resistivity is negative within a wide current range $0.07<\varepsilon_j<0.42$ before it becomes positive with further increasing current density. This may provide a possible explanation for the zero-differential resistance state recently observed at quite small dc bias in impure samples.[33]

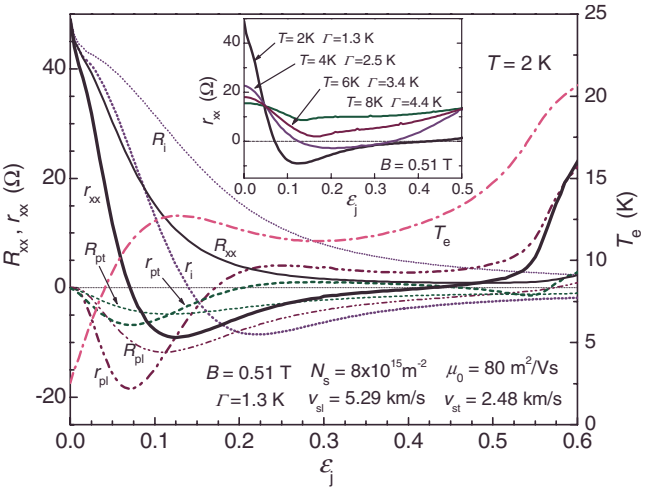

FIG. 5. (Color online) Absolute R_{xx} and differential r_{xx} resistivities and their respective contributions from impurity, LA phonons, and TA phonons (R_i and r_i, $R_{\rm pl}$ and $r_{\rm pl}$, and $R_{\rm pt}$ and $r_{\rm pt}$) and the electron temperature T_e are shown versus ε_j at a lattice temperature T=2 K and a magnetic field B=0.51 T for a GaAs-based heterosystem. The inset plots r_{xx} at T=2, 4, 6, and 8 K with corresponding half-width of the Landau level Γ.

As an important parameter in the present analysis, the half-width Γ of the Landau level, or the single particle lifetime or $\tau_s=1/2\Gamma$ of the electron in the magnetic field, which depends on all kinds of elastic and inelastic scatterings induced by electron-impurity, electron-phonon, and electron-electron interactions in the system, is temperature T dependent. At fixed B field, Γ certainly increases with increasing temperature due to enhanced electron-phonon and electron-electron scatterings. With this in consideration, the sharp drop in differential resistivity r_{xx} at T=2 K rapidly disappears when increasing temperature, as shown in the inset of Fig. 5, which is calculated with enlarged Γ at T=4, 6, and 8 K.

VI. SUMMARY

In summary, we have examined magnetophonon resonances in GaAs-based 2D systems at low temperatures. Good agreement between theoretical prediction and experimental observation is obtained by using the well-defined bulk LA and TA phonon modes with no adjustable parameter. We find that a finite dc excitation can not only greatly enhance the phonon resistivity by heating the electron gas, but can also induce additional and prominent phonon resonance peaks, which give rise to remarkable resistance oscillations and negative differential resistivity in nonlinear transport.

ACKNOWLEDGMENTS

This work was supported by the projects of the National Science Foundation of China and the Shanghai Municipal Commission of Science and Technology.

[1] V. I. Ryzhii, Sov. Phys. Solid State **11**, 2078 (1970).
[2] R. G. Mani, J. H. Smet, K. von Klitzing, V. Narayanamurti, W. B. Johnson, and V. Umansky, Nature (London) **420**, 646 (2002).
[3] M. A. Zudov, R. R. Du, L. N. Pfeiffer, and K. W. West, Phys. Rev. Lett. **90**, 046807 (2003).
[4] A. C. Durst, S. Sachdev, N. Read, and S. M. Girvin, Phys. Rev. Lett. **91**, 086803 (2003).
[5] X. L. Lei and S. Y. Liu, Phys. Rev. Lett. **91**, 226805 (2003).
[6] J. Dietel, L. I. Glazman, F. W. J. Hekking, and F. von Oppen, Phys. Rev. B **71**, 045329 (2005).
[7] M. Torres and A. Kunold, Phys. Rev. B **71**, 115313 (2005).
[8] I. A. Dmitriev, M. G. Vavilov, I. L. Aleiner, A. D. Mirlin, and D. G. Polyakov, Phys. Rev. B **71**, 115316 (2005).
[9] J. Iñarrea and G. Platero, Phys. Rev. Lett. **94**, 016806 (2005).
[10] C. L. Yang, J. Zhang, R. R. Du, J. A. Simmons, and J. L. Reno, Phys. Rev. Lett. **89**, 076801 (2002).
[11] A. A. Bykov, J. Q. Zhang, S. Vitkalov, A. K. Kalagin, and A. K. Bakarov, Phys. Rev. B **72**, 245307 (2005).
[12] W. Zhang, H.-S. Chiang, M. A. Zudov, L. N. Pfeiffer, and K. W. West, Phys. Rev. B **75**, 041304(R) (2007).
[13] J. Zhang, S. Vitkalov, A. A. Bykov, A. K. Kalagin, and A. K. Bakarov, Phys. Rev. B **75**, 081305(R) (2007).
[14] X. L. Lei, Appl. Phys. Lett. **90**, 132119 (2007).
[15] M. G. Vavilov, I. L. Aleiner, and L. I. Glazman, Phys. Rev. B **76**, 115331 (2007).
[16] J. Iñarrea, Appl. Phys. Lett. **91**, 222107 (2007).
[17] A. Kunold and M. Torres, arXiv:0707.2396 (unpublished).
[18] V. L. Gurevich and Y. Firsov, Sov. Phys. JETP **13**, 137 (1961).
[19] D. C. Tsui, Th. Englert, A. Y. Cho, and A. C. Gossard, Phys. Rev. Lett. **44**, 341 (1980).
[20] M. A. Zudov, I. V. Ponomarev, A. L. Efros, R. R. Du, J. A. Simmons, and J. L. Reno, Phys. Rev. Lett. **86**, 3614 (2001).
[21] I. V. Ponomarev and A. L. Efros, Phys. Rev. B **63**, 165305 (2001).
[22] C. L. Yang, M. A. Zudov, J. Zhang, R. R. Du, J. A. Simmons, and J. L. Reno, Physica E (Amsterdam) **12**, 443 (2002).
[23] A. A. Bykov, A. K. Kalagin, and A. K. Bakarov, JETP Lett. **81**, 523 (2005).
[24] W. Zhang, M. A. Zudov, L. N. Pfeiffer, and K. W. West, Phys. Rev. Lett. **100**, 036805 (2008).
[25] C. S. Ting, S. C. Ying, and J. J. Quinn, Phys. Rev. B **14**, 4439 (1976); **16**, 5394 (1977).
[26] X. L. Lei and C. S. Ting, Phys. Rev. B **30**, 4809 (1984); **32**, 1112 (1985).
[27] X. L. Lei, J. L. Birman, and C. S. Ting, J. Appl. Phys. **58**, 2270 (1985).
[28] W. Cai, X. L. Lei, and C. S. Ting, Phys. Rev. B **31**, 4070 (1985); X. L. Lei, W. Cai, and C. S. Ting, J. Phys. C **18**, 4315 (1985).
[29] T. Ando, A. B. Fowler, and F. Stern, Rev. Mod. Phys. **54**, 437 (1982).
[30] H. Scher and T. Holstein, Phys. Rev. **148**, 598 (1966).
[31] J. Zhang, S. K. Lyo, R. R. Du, J. A. Simmons, and J. L. Reno, Phys. Rev. Lett. **92**, 156802 (2004).
[32] X. L. Lei and S. Y. Liu, Phys. Rev. B **72**, 075345 (2005).
[33] A. A. Bykov, J. Q. Zhang, S. Vitkalov, A. K. Kalagin, and A. K. Bakarov, Phys. Rev. Lett. **99**, 116801 (2007).